J|A|C|S
ARTICLES

Published on Web 08/13/2009

Long-Term Improvements to Photoluminescence and Dispersion Stability by Flowing SDS-SWNT Suspensions through Microfluidic Channels

Carlos A. Silvera-Batista,[†] Philip Weinberg,[†] Jason E. Butler,[†] and Kirk J. Ziegler*[,†,‡,§]

Department of Chemical Engineering, Department of Materials Science and Engineering, and Center for Surface Science and Engineering, University of Florida, Gainesville, Florida 32611

Received May 7, 2009; E-mail: kziegler@che.ufl.edu

Abstract: Shearing single-walled carbon nanotubes (SWNTs) coated with sodium dodecyl sulfate in microfluidic channels significantly increases the photoluminescence (PL) intensity and dispersion stability of SWNTs. The PL quantum yield (QY) of SWNTs improves by a factor of 3 for initially bright suspensions; on the other hand, SWNT QYs in a "poor" suspension improve by 2 orders of magnitude. In both cases, the QYs of the sheared suspensions are approximately 1%. The increases in PL intensity persist for months and are most prominent in larger diameter SWNTs. These improvements are attributed to surfactant reorganization rather than disaggregation of SWNTs bundles or shear-induced alignment. The results also highlight potential opportunities to eliminate discrepancies in the PL intensity of different suspensions and further improve the PL of SWNTs by tailoring the surfactant structure around SWNTs.

Introduction

Since the discovery of single-walled carbon nanotubes (SWNTs), researchers have envisioned many applications that take advantage of their astounding physical properties.[1] However, dispersing and separating as-grown SWNTs remains a significant impediment to their use in most applications.[2] Dispersion and separation of SWNTs are inherently linked since no separation by type can occur without adequate dispersion of individual SWNTs. A significant milestone was the dispersion of SWNTs in aqueous suspensions with the aid of surfactants.[3] Most work has focused on the use of sodium dodecyl sulfate (SDS), sodium dodecylbenzene sulfonate (SDBS), and sodium cholate (SC), although multiple surfactants have been used.[4−6]

The dispersion of SWNTs enables (*n*,*m*) type characterization through absorbance and photoluminescence (PL).[7,8] The PL emission is often used to quantify separations of semiconducting SWNTs.[9−11] However, the effect of the surfactant and surrounding environment is still not well understood.[12−14] For example, different intensities and quantum yields are obtained when suspended by different surfactants or by different research groups.[5,6,15] These differences in intensity have been attributed to differences in dispersion[16] or extrinsic environmental effects. The optically excited electronic states of SWNTs are highly mobile,[17] making them sensitive to extrinsic effects that reduce PL intensity, including the state of aggregation,[18−21] polarizability of the surrounding environment,[14,22] pH of the suspension,[17,23,24]

[†] Department of Chemical Engineering.
[‡] Department of Materials Science and Engineering.
[§] Center for Surface Science and Engineering.

(1) Baughman, R. H.; Zakhidov, A. A.; de Heer, W. A. *Science* **2002**, *297*, 787.
(2) Hu, H.; Yu, A.; Kim, E.; Zhao, B.; Itkis, M. E.; Bekyarova, E.; Haddon, R. C. *J. Phys. Chem. B* **2005**, *109*, 11520.
(3) O'Connell, M. J.; Bachilo, S. M.; Huffman, C. B.; Moore, V. C.; Strano, M. S.; Haroz, E. H.; Rialon, K. L.; Boul, P. J.; Noon, W. H.; Kittrell, C.; Ma, J. P.; Hauge, R. H.; Weisman, R. B.; Smalley, R. E. *Science* **2002**, *297*, 593.
(4) Bandyopadhyaya, R.; Nativ-Roth, E.; Regev, O.; Yerushalmi-Rozen, R. *Nano Lett.* **2002**, *2*, 25.
(5) Haggenmueller, R.; Rahatekar, S. S.; Fagan, J. A.; Chun, J. H.; Becker, M. L.; Naik, R. R.; Krauss, T.; Carlson, L.; Kadla, J. F.; Trulove, P. C.; Fox, D. F.; DeLong, H. C.; Fang, Z. C.; Kelley, S. O.; Gilman, J. W. *Langmuir* **2008**, *24*, 5070.
(6) Moore, V. C.; Strano, M. S.; Haroz, E. H.; Hauge, R. H.; Smalley, R. E.; Schmidt, J.; Talmon, Y. *Nano Lett.* **2003**, *3*, 1379.
(7) Bachilo, S. M.; Strano, M. S.; Kittrell, C.; Hauge, R. H.; Smalley, R. E.; Weisman, R. B. *Science* **2002**, *298*, 2361.
(8) Weisman, R. B.; Bachilo, S. M. *Nano Lett.* **2003**, *3*, 1235.
(9) Chen, F.; Wang, B.; Chen, Y.; Li, L.-J. *Nano Lett.* **2007**, *7*, 3013.
(10) Hwang, J. Y.; Nish, A.; Doig, J.; Douven, S.; Chen, C. W.; Chen, L. C.; Nicholas, R. J. *J. Am. Chem. Soc.* **2008**, *130*, 3543.
(11) Niyogi, S.; Boukhalfa, S.; Chikkannanavar, S. B.; McDonald, T. J.; Heben, M. J.; Doorn, S. K. *J. Am. Chem. Soc.* **2007**, *129*, 1898.
(12) Dukovic, G.; White, B. E.; Zhou, Z. Y.; Wang, F.; Jockusch, S.; Steigerwald, M. L.; Heinz, T. F.; Friesner, R. A.; Turro, N. J.; Brus, L. E. *J. Am. Chem. Soc.* **2004**, *126*, 15269.
(13) Tsyboulski, D. A.; Rocha, J. D. R.; Bachilo, S. M.; Cognet, L.; Weisman, R. B. *Nano Lett.* **2007**, *7*, 3080.
(14) Wang, R. K.; Chen, W.-C.; Campos, D. K.; Ziegler, K. J. *J. Am. Chem. Soc.* **2008**, *130*, 16330.
(15) Islam, M. F.; Rojas, E.; Bergey, D. M.; Johnson, A. T.; Yodh, A. G. *Nano Lett.* **2003**, *3*, 269.
(16) Okazaki, T.; Saito, T.; Matsuura, K.; Ohshima, S.; Yumura, M.; Iijima, S. *Nano Lett.* **2005**, *5*, 2618.
(17) Cognet, L.; Tsyboulski, D. A.; Rocha, J. D. R.; Doyle, C. D.; Tour, J. M.; Weisman, R. B. *Science* **2007**, *316*, 1465.
(18) Crochet, J.; Clemens, M.; Hertel, T. *J. Am. Chem. Soc.* **2007**, *129*, 8058.
(19) Qian, H.; Araujo, P. T.; Georgi, C.; Gokus, T.; Hartmann, N.; Green, A. A.; Jorio, A.; Hersam, M. C.; Novotny, L.; Hartschuh, A. *Nano Lett.* **2008**, *8*, 2706.
(20) Tan, P. H.; Rozhin, A. G.; Hasan, T.; Hu, P.; Scardaci, V.; Milne, W. I.; Ferrari, A. C. *Phys. Rev. Lett.* **2007**, *99*, 137402.
(21) Torrens, O. N.; Milkie, D. E.; Zheng, M.; Kikkawa, J. M. *Nano Lett.* **2006**, *6*, 2864.
(22) Choi, J. H.; Strano, M. S. *Appl. Phys. Lett.* **2007**, *90*, 223114.

surface reactions,[12,17,25,26] sidewall defects,[13,17,19,27,28] surfactant inhomogeneties,[13,19,27,29] electric fields,[30] and the length of SWNTs.[31,32]

Single-molecule studies of SWNTs have been important in identifying and characterizing the effects of extrinsic factors on PL. Fluctuations in PL emission intensity along the length of nanotubes has been observed in both aqueous solutions[13] and air.[28] These dark spots allowed Cognet et al.[17] to estimate the exciton diffusion length to be approximately 90 nm. In SWNTs that have uniform PL intensity, quantum yields (QYs) are estimated to be 7−8%.[13,28] These measurements surpass previous ensemble estimates of QY (0.1−1%).[3,29,33] Therefore, the presence of extrinsic factors may help explain the discrepancy between bulk and single-molecule measurements of SWNT QY.

It is becoming increasingly clear that SWNT−surfactant and surfactant−surfactant interactions are important in defining both dispersion and PL properties.[14,23,34,35] Three models of surfactant assembly on SWNT sidewalls have been suggested: hemimicellar,[15] cylindrical,[3] and assemblies characterized by lack of long-range order.[36] However, a recent simulation study suggests the latter model may be the most appropriate.[35] This study shows that surfactant molecules do not present long-range order around SWNTs and large portions of the nanotube sidewall may be exposed to water. This has important implications on the PL emission intensity since several researchers have demonstrated the quenching effects of protons or water,[17,24,29] indicating that PL emission of SWNTs may depend on both extrinsic factors and processes that alter the surfactant structure.

Researchers have determined that processing conditions have a significant impact on the PL emission.[37] The ultimate objective is to compensate for these differences.[5,13] Differences in surfactant structure, as highlighted by recent simulations,[35,38] may help explain the discrepancies in PL emission observed between surfactants and by different research groups for the same surfactant.[5,6,15] Some researchers already have developed processes to control the surfactant structure around SWNTs, including in situ polymerization of polyvinylpyrrolidone (PVP),[23] electrolyte tuning,[34] and combining surfactants for density gradient centrifugation.[39] Our group recently demonstrated that organic solvents can alter the surfactant shell around SWNTs.[14] Here we explore the effect of SWNT processing, such as flow through microchannels,[40−42] on the surfactant structure and PL emission of SWNTs. The high shear environment in the channel results in significant increases in PL intensity after flowing through the channel. These changes persist for months and cannot be attributed to shear-induced alignment[43] or disaggregation. Photoluminescence, absorbance, and Raman spectroscopy suggest that shearing a SWNT suspension helps anneal the surfactant shell around the nanotube. The altered surfactant structure enhances the stability of the suspension and improves the PL intensity, especially for the largest diameter SWNTs. We also demonstrate that this process can eliminate discrepancies in the PL intensity of different suspensions.

Methods

Dispersion. Nanotube suspensions were prepared with 60 mg of SWNTs (Rice HPR 162.3) and mixed with 200 mL of a 1 wt % SDS aqueous solution. SDS was purchased from Sigma-Aldrich and used as received. The suspension was then mixed with a high-shear homogenizer (IKA T-25 Ultra-Turrax) at 13,000 rpm for 2 h and ultrasonicated in a cuphorn (Misonix S3000) at 130 W for 10 min. Subsequently, the suspension was ultracentrifuged at 20,000 rpm (Beckman Coulter Optima L-80 K) for 5 h to remove nanotube bundles.

Microchannel Fabrication. Microfluidic channels were fabricated using soft lithography[44] with poly(dimethylsiloxane) (PDMS) as the structural material. Briefly, a 4 in. silicon wafer was patterned with the negative photoresist SU-8 2015 (Microchem) using a printed transparency as the shadow mask. A 1/10 ratio mixture of PDMS curing agent and base (Sylgard 184; Dow Corning) was poured over the patterned silicon wafer and cured by heating at 353 K for 2 h. The cured PDMS was peeled off from the silicon wafer and diced to obtain individual chips. The channels were bonded irreversibly to glass slides by bringing the channel and the glass slide into intimate contact after a brief treatment of the PDMS chips with oxygen plasma (Anatech SCE600 Asher). The channels were 2 cm long with a cross sectional area of $20 \times 60\ \mu m^2$.

Shearing of SWNT Suspensions. The SWNT suspensions were sheared using a Couette geometry in an ARES LS-1 strain-controlled rheometer (TA Instruments). The maximum attainable shear rate in the rheometer was 4000 s^{-1}. For each shear rate, the suspensions were sheared for 5 min. On the other hand, mean rates of shear as high as $1.72 \times 10^5\ s^{-1}$ were achieved by flowing the suspension through microchannels at different flow rates. A syringe pump (Pump 11 Pico Plus; Harvard Apparatus) was used to control the flow of the SWNT suspension through the microchannel with flow rates between 5 and 4000 μL/h. It is important to remark that the rate of failure of the channel increases rapidly when the flow rate is higher than 2500 μL/h. Forward, reverse, and random sweeps of the shear rate were used to verify that the observed spectral changes at a given shear rate were not due to preshearing within the tubing leading to the microfluidic channel. The intensity versus shear rate data was collected from 15 different suspensions, and three experiments were performed at each shear rate for all suspensions.

(23) Duque, J. G.; Cognet, L.; Parra-Vasquez, A. N. G.; Nicholas, N.; Schmidt, H. K.; Pasquali, M. *J. Am. Chem. Soc.* **2008**, *130*, 2626.
(24) Strano, M. S.; Huffman, C. B.; Moore, V. C.; O'Connell, M. J.; Haroz, E. H.; Hubbard, J.; Miller, M.; Rialon, K.; Kittrell, C.; Ramesh, S.; Hauge, R. H.; Smalley, R. E. *J. Phys. Chem. B* **2003**, *107*, 6979.
(25) Doyle, C. D.; Rocha, J. D. R.; Weisman, R. B.; Tour, J. M. *J. Am. Chem. Soc.* **2008**, *130*, 6795.
(26) Nish, A.; Nicholas, R. J. *Phys. Chem. Chem. Phys.* **2006**, *8*, 3547.
(27) Gokus, T.; Hartschuh, A.; Harutyunyan, H.; Allegrini, M.; Hennrich, F.; Kappes, M.; Green, A. A.; Hersam, M. C.; Araujo, P. T.; Jorio, A. *Appl. Phys. Lett.* **2008**, *92*, 153116.
(28) Lefebvre, J.; Austing, D. G.; Bond, J.; Finnie, P. *Nano Lett.* **2006**, *6*, 1603.
(29) Blackburn, J. L.; McDonald, T. J.; Metzger, W. K.; Engtrakul, C.; Rumbles, G.; Heben, M. J. *Nano Lett.* **2008**, *8*, 1047.
(30) Naumov, A. V.; Bachilo, S. M.; Tsyboulski, D. A.; Weisman, R. B. *Nano Lett.* **2008**, *8*, 1527.
(31) Fagan, J. A.; Simpson, J. R.; Bauer, B. J.; Lacerda, S. H. D.; Becker, M. L.; Chun, J.; Migler, K. B.; Walker, A. R. H.; Hobbie, E. K. *J. Am. Chem. Soc.* **2007**, *129*, 10607.
(32) Heller, D. A.; Mayrhofer, R. M.; Baik, S.; Grinkova, Y. V.; Usrey, M. L.; Strano, M. S. *J. Am. Chem. Soc.* **2004**, *126*, 14567.
(33) Jones, M.; Engtrakul, C.; Metzger, W. K.; Ellingson, R. J.; Nozik, A. J.; Heben, M. J.; Rumbles, G. *Phys. Rev. B* **2005**, *71*, 115426.
(34) Niyogi, S.; Densmore, C. G.; Doorn, S. K. *J. Am. Chem. Soc.* **2009**, *131*, 1144.
(35) Tummala, N. R.; Striolo, A. *ACS Nano* **2009**, *3*, 595.
(36) Yurekli, K.; Mitchell, C. A.; Krishnamoorti, R. J. *J. Am. Chem. Soc.* **2004**, *126*, 9902.
(37) Heller, D. A.; Barone, P. W.; Strano, M. S. *Carbon* **2005**, *43*, 651.
(38) Wallace, E. J.; Sansom, M. S. P. *Nano Lett.* **2007**, *7*, 1923.
(39) Arnold, M. S.; Green, A. A.; Hulvat, J. F.; Stupp, S. I.; Hersam, M. C. *Nat. Nanotechnol.* **2006**, *1*, 60.
(40) Mattsson, M.; Gromov, A.; Dittmer, S.; Eriksson, E.; Nerushev, O. A.; Campbell, E. E. B. *J. Nanosci. Nanotechnol.* **2007**, *7*, 3431.
(41) Peng, H. Q.; Alvarez, N. T.; Kittrell, C.; Hauge, R. H.; Schmidt, H. K. *J. Am. Chem. Soc.* **2006**, *128*, 8396.
(42) Shin, D. H.; Kim, J. E.; Shim, H. C.; Song, J. W.; Yoon, J. H.; Kim, J.; Jeong, S.; Kang, J.; Baik, S.; Han, C. S. *Nano Lett.* **2008**, *8*, 4380.
(43) Casey, J. P.; Bachilo, S. M.; Moran, C. H.; Weisman, R. B. *ACS Nano* **2008**, *2*, 1738.
(44) Xia, Y. N.; Whitesides, G. M. *Annu. Rev. Mater. Sci.* **1998**, *28*, 153.

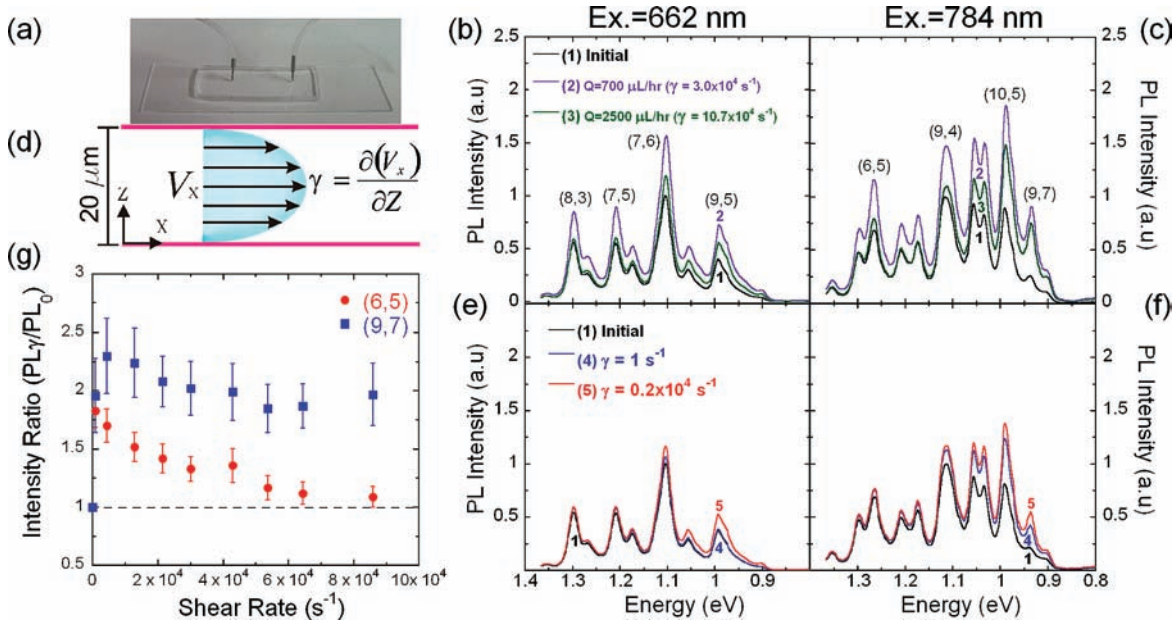

Figure 1. (a) PDMS microchannels used to shear SDS-SWNT suspensions. PL emission spectra from SWNTs that flowed through the microfluidic channels are shown for different flow rates (or mean shear rates) with (b) 662 and (c) 784 nm excitation. (d) Cartoon representing the parabolic velocity profile and shearing of the suspension flowing through the microchannel. PL emission spectra are shown for SDS-SWNT suspensions sheared in a rheometer using a Couette geometry with (e) 662 and (f) 784 nm excitation. (g) The intensity of the (6,5) and (9,7) SWNT species at each shear rate in the microchannel is normalized by its intensity in the initial (nonsheared) sample (PL_γ/PL_0) and plotted as a function of shear rate.

Dielectrophoresis. The electrodes were fabricated using the lift-off technique. Briefly, a 100 nm layer of Au was sputtered on a glass slide that was previously patterned with the AZ 9260 photoresist. A 10 nm layer of Cr was used as the adhesion layer. After metal deposition, the electrodes were obtained by dipping the glass slide in acetone to remove the photoresist. A droplet of the SWNT suspension was cast onto the electrodes, and then an electric field (10 $V_{p\text{-}p}$, 10 MHz) was applied for 1 min to minimize solvent evaporation. The droplet was blown off with a stream of nitrogen gas, and the substrate was rinsed with ethanol and deionized water to remove the surfactant from the deposited SWNTs. The deposited SWNTs were then analyzed with Raman spectroscopy.

Characterization. All SWNT suspensions were characterized by vis-NIR absorbance and NIR-fluorescence spectroscopy using an Applied NanoFluorescence Nanospectrolyzer (Houston, TX) with excitation from 662 and 784 nm diode lasers. A minimum of 200 μL of SWNT suspension was needed to analyze the effluent from the microchannel. Two or three channels were used in parallel to reduce the experimental time when using small flow rates (shear rates). Raman spectra were recorded using a Renishaw Invia Bio Raman with excitation from a 785 nm diode laser.

Results

Suspensions of SDS-coated SWNTs were pumped through microfluidic channels, such as those shown in Figure 1a, at different rates of flow. The effluent was collected and characterized with fluorescence and absorption spectroscopy. The PL emission spectra for the initial SDS-SWNT suspensions shown in Figures 1b and 1c present high-intensity and well-defined peaks due to E_{11} transitions from specific (n,m) SWNT types, which are characteristic of well-dispersed semiconducting SWNTs. After processing the SWNT suspensions through the microfluidic channel, the intensity of the emission peaks increases significantly as shown in Figures 1b and 1c. These increases in intensity depend on the flow rate while the peak width does not change.

The pressure-driven flow through the microfluidic channel generates high rates of shear as shown in Figure 1d. The mean rate of shear is approximately 3.0×10^4 and 10.7×10^4 s^{-1} for the flow rates of 700 and 2500 μL/h, respectively. The SWNT suspensions were also sheared in a rheometer using a Couette geometry. Shearing at a rate of 1 s^{-1} changed the PL emission intensity marginally, as shown in Figures 1e and 1f. However, a larger intensity change is observed when shearing at 0.2×10^4 s^{-1}.

A direct comparison of PL intensities of SWNTs processed in the microfluidic channel and the rheometer cannot be made. Within the Couette cell, only a small fraction of the fluid volume resides in the shearing gap; hence, most of the SWNTs do not experience any shear. Nonetheless, the increase in intensity qualitatively supports the concept that shear affects the PL emission.

In both shearing experiments, the SWNTs with the smallest diameters (e.g., (6,5) types) show small intensity increases, whereas the peaks of the nanotubes having the largest diameters (e.g., (9,7) types), which are predominantly excited at 784 nm (Figure 1c), show more significant increases. The changes in PL emission intensity of the (6,5) and (9,7) SWNT types are plotted in Figure 1g over a wide range of shear rates. The PL intensity of each (n,m) type (normalized by its initial emission intensity) is usually greater following shear. As seen in Figure 1g, the emission intensity of the (9,7) nanotubes can more than double after shearing. Most (n,m) types also show a well-defined maximum in the PL intensity. Although the positions of the maxima vary with each suspension and SWNT type, it is typically located at $\sim 10^4$ s^{-1}. The PL intensity then slowly decays as higher shear rates are applied until it plateaus at approximately 3×10^4 s^{-1} for the SWNTs of larger diameter. For small diameter SWNTs at large shear rates, the intensity of the sheared suspension can be equal to or lower than the intensity of the initial suspension. Note that increasing the mean

rate of shear simultaneously decreases the residence time of SWNTs in the microchannel; consequently, the observations of the changes in PL intensity may depend on not only the mean shear rate but also the length of the channel. However, experiments investigating the effect of residence time have yet to be performed.

Discussion

Shear-Induced Alignment. SWNTs are highly anisotropic particles with optical transitions that are highly polarized along the nanotube main axis.[45] The optical anisotropy of SWNTs has been studied by aligning nanotubes with mechanical stretching of polymer films,[46] electric fields,[47] and fluid flow.[48] Weisman and co-workers used the optical anisotropy of SWNTs to measure length distributions as the nanotubes were aligned by shear flow.[43] The authors reported emission intensities that doubled as the nanotubes aligned in the suspension. Similarly, SWNTs processed in the rheometer or microfluidic channels could also align under the applied shear. However, the PL emission from the suspensions in Figure 1 were measured after collecting at least 200 μL of the suspension from the microfluidic channels, which took several hours for some shear rates (flow rates).

These suspensions are dilute according to the criteria of Doi and Edwards since $nL^3 \approx 0.6$, where n is the number density and L is the average length of the SWNTs. Consequently, the time required for Brownian forces to randomize the orientations of the ensemble of aligned nanotubes scales with the inverse rotational diffusivity, $1/D_r$,[49] of a single rod. Though suspended in a dilute solution of surfactants, the rotational diffusivity of the SWNTs is modeled as rigid rods of high aspect ratio suspended in a Newtonian fluid[49] to give

$$D_r = \frac{3k_BT\ln(2L/d)}{\pi\mu L^3}$$

where k_BT is the thermal energy, μ is the viscosity of the fluid media (0.001 Pa·s for water), and d is the effective diameter of the rod.[50,51] Assuming a value between 2 and 5 nm for the effective diameter (including surfactant shell) and 500 nm for the length of a nanotube, a randomization time of $10/D_r$ is estimated to fall between 51 and 60 ms at room temperature.[51−53] The PL spectra were typically measured more than 2 h after shearing, and as discussed further below, the increases in PL intensity persist for weeks. Hence, alignment is not responsible for the increases in PL intensity of SWNTs after shearing.

Disaggregation of SWNT Bundles. The creation of additional, isolated SWNTs from the shear-induced break-up of bundles is one possible explanation for the increase in PL intensity after shearing. However, no significant changes are observed to either the absorbance or Raman spectra, which probe the aggregation state of SWNT suspensions. Figure 2a shows the vis-NIR absorbance spectra of SWNT suspensions sheared at rates corresponding to the maximum and plateau regions in Figure 1g. The spectra show that the absorbance changes after shearing

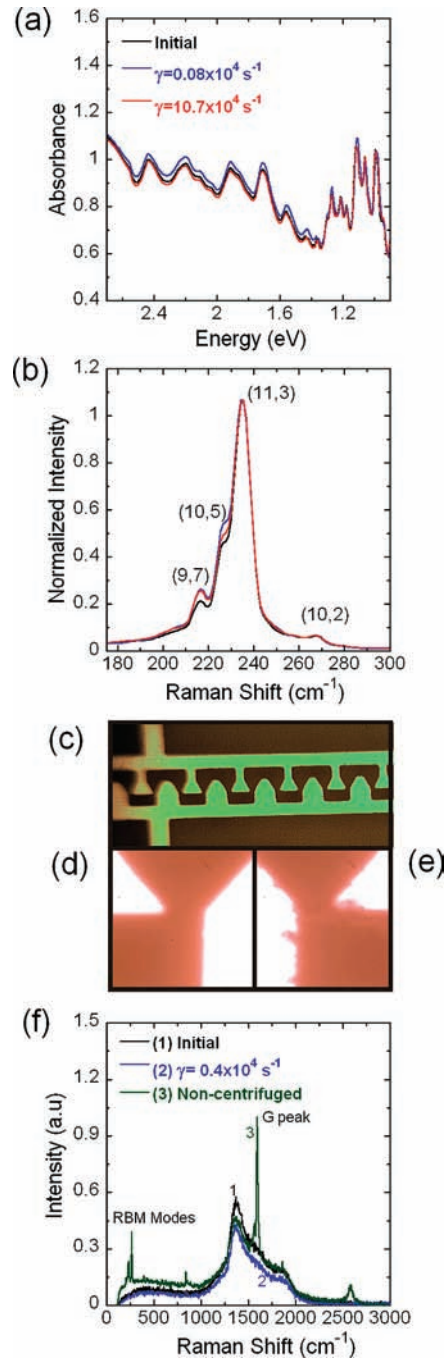

Figure 2. (a) Absorbance and (b) Raman RBM spectra (ex = 785 nm) of a SWNT suspension after shearing at average rates of 0.08×10^4 and 10.7×10^4 s^{-1}. The Raman spectra are normalized to the G peak. (c) Digital image of the electrodes used for dielectrophoretic deposition of SWNTs. Digital images of the electrodes (50×) after deposition from (d) sheared and (e) noncentrifuged suspensions. The shear rate (0.4×10^4 s^{-1}) was chosen where the suspension showed the maximum intensity increases. Notice the aggregates of SWNTs after deposition of the noncentrifuged suspension in (e). (f) Raman spectra (ex = 785 nm) of the initial, sheared, and noncentrifuged SWNT suspensions deposited on the electrodes by dielectrophoresis. The excitation wavelength only probes semiconducting SWNTs.

(45) Lefebvre, J.; Fraser, J. M.; Finnie, P.; Homma, Y. *Phys. Rev. B* **2004**, *69*, 075403.
(46) Kim, Y.; Minami, N.; Kazaoui, S. *Appl. Phys. Lett.* **2005**, *86*, 073103.
(47) Fagan, J. A.; Simpson, J. R.; Landi, B. J.; Richter, L. J.; Mandelbaum, I.; Bajpai, V.; Ho, D. L.; Raffaelle, R.; Walker, A. R. H.; Bauer, B. J.; Hobbie, E. K. *Phys. Rev. Lett.* **2007**, *98*, 147402.
(48) Fry, D.; Langhorst, B.; Kim, H.; Grulke, E.; Wang, H.; Hobbie, E. K. *Phys. Rev. Lett.* **2005**, *95*, 038304.
(49) Doi, M.; Edwards, S. F. *The Theory of Polymer Dynamics*; Oxford University Press: New York, 1986.
(50) Duggal, R.; Pasquali, M. *Phys. Rev. Lett.* **2006**, *96*, 246104.
(51) Tsyboulski, D. A.; Bachilo, S. M.; Kolomeisky, A. B.; Weisman, R. B. *ACS Nano* **2008**, *2*, 1770.
(52) Arnold, M. S.; Suntivich, J.; Stupp, S. I.; Hersam, M. C. *ACS Nano* **2008**, *2*, 2291.
(53) Richard, C.; Balavoine, F.; Schultz, P.; Ebbesen, T. W.; Mioskowski, C. *Science* **2003**, *300*, 775.

are minor (less than ~5%) at any shear rate. Slight peak shifts are observed in some sheared SWNT suspensions; however, these changes were not systematic. Further, the peak shifts are often red-shifted as shown for the spectra corresponding to SWNT suspensions sheared at 0.08×10^4 s^{-1} in Figure 2a. Red shifts typically indicate that the suspension has aggregated.[3] However, this suspension exhibits some of the highest PL intensity increases as shown in Figure 1g.

The normalized Raman spectra of the SWNT radial breathing modes (RBMs) also show no evidence of changes to the aggregation state after shearing as shown in Figure 2b. The RBM peak for the (10,2) SWNT type is very sensitive to aggregation and shifts to ~270 cm^{-1} when bundled with other nanotubes. Therefore, this peak provides a measure of the degree of aggregation in SWNT suspensions.[54] As seen in Figure 2b, the aggregation peak has no changes at any shear rate. There is a small increase in the intensity of the RBM modes from the (10,5) and (9,7) nanotubes, whereas the intensity of the (11,3) nanotubes remains constant. The intensity increases of the (10,5) and (9,7) nanotubes follow a similar trend as seen in Figure 1g with the highest intensity occurring after moderate shear rates. These increases could indicate some changes to the aggregation state; however, researchers have shown the intensity of the (11,3) SWNT should increase more significantly than either of these SWNT types if bundles are separated into individual SWNTs.[55] The fact that the RBM intensity from the (11,3) SWNT remains constant and the other SWNTs show only slight increases in intensity suggests that if disaggregation occurs, it must be a minor effect. The intensity of the RBMs is also sensitive to quenching effects[24] and will be discussed further below.

To probe the aggregation state further, the dielectrophoresis procedure developed by Kumatani and Warburton was used to characterize the suspensions.[56] The frequency (10 MHz) of the applied electric field is chosen so metallic SWNTs are attracted to the electrodes while semiconductors are repelled or experience a much smaller attractive force.[57] Hence, semiconducting SWNTs are deposited on the electrodes only if aggregated with metallic SWNTs, as shown in Figure 2c−e. After deposition of a noncentrifuged sample, large aggregates are evident on the electrodes (Figure 2e). The extent of aggregation can then be measured by selectively probing the semiconducting SWNTs with Raman spectroscopy. The Raman spectra of SWNTs deposited from the initial (no shear), sheared ($\gamma = 0.4 \times 10^4$ s^{-1}), and noncentrifuged SWNT suspensions are shown in Figure 2f. As expected, the Raman spectra for noncentrifuged suspensions containing bundled SWNTs show very strong RBM and G peaks typical of deposited semiconducting SWNTs. On the other hand, the RBM and G peaks are absent from both the initial and sheared SWNT suspensions. Once again, these results suggest the initial SDS-SWNT suspensions are well-dispersed and the state of aggregation does not change significantly after flowing through the microchannel.

Fluid Flow Segregation or Removal of Impurities. Researchers have observed that shear flow within a confining geometry can segregate semidilute suspensions of carbon nanotubes by length.[48] If segregation were occurring in the microfluidic channels, the PL intensity of the SWNT suspensions could be affected by nonlinear changes to the quantum yields of nanotubes as a function of length.[58,59] However, development of the length-dependent distribution for a dilute suspension of Brownian rods requires a large residence time.[60] Estimates based upon the parameters for these experiments indicate that the rods would have to reside within the channel for at least 90 s, whereas the actual residence time is 1 s at most. Therefore, it is unlikely that segregation occurs under these flow conditions. In addition, similar PL intensity increases are observed in channels with different dimensions, a critical parameter that would affect the segregation if occurring. Furthermore, no evidence of SWNT removal in either the channel or in the absorbance spectra (see Figure 2a) is observed.

Similar arguments would suggest that the removal of other impurities, such as metal catalysts, fullerenes, and other carbonaceous material would be minimal. This is further supported by inductively coupled plasma atomic emission spectrometry (ICP-AES), which shows that the amount of iron in the suspension does not change after flowing through the microchannel (not shown). While selective interaction with the walls of the channel could occur, the rheology data in Figures 1e and 1f still show PL increases. Channels constructed of glass/paraffin also showed similar PL intensity increases, ruling out selective interaction with the channel walls.

Surfactant Reorganization. Another plausible explanation for the increase in PL intensity of specific (*n*,*m*) SWNT types is the rearrangement of the surfactant shell surrounding the nanotubes. Our group recently demonstrated the ability to manipulate the SDS shell surrounding SWNTs using immiscible organic solvents.[14] After mixing with organic solvents and allowing it to evaporate, the surfactant assumed a conformation that provided better protection to extrinsic quenching events, such as protons.[12,14,17,23,24,29] This chemical "annealing" process was found to increase the PL intensity of the largest diameter SWNTs by as much as 175% without changes to either absorbance or Raman spectra. In addition, Doorn and collaborators recently reported that the addition of salts to SDS-SWNT suspensions can alter the surfactant structure surrounding the nanotubes, resulting in increases of PL intensity as well as narrowing of spectral line width of SWNT species.[34] In a similar fashion, the shear applied to SWNT suspensions from either microfluidic channels or a rheometer may also rearrange the surfactant structure, resulting in reduced quenching from extrinsic factors. In fact, shear has been shown to cause phase transitions and induce changes in the self-assembling properties of micellar systems.[61,62] For example, micelles of CTAT (cetyl trimethylammonium *p*-toluenesulphonate), which are cylindrical, can grow when sheared and return to the initial state once shearing has stopped.[63]

If shear can improve the ability of the surfactant to protect SWNTs from quenching protons, the suspension should maintain

(54) Heller, D. A.; Barone, P. W.; Swanson, J. P.; Mayrhofer, R. M.; Strano, M. S. *J. Phys. Chem. B* **2004**, *108*, 6905.
(55) Strano, M. S.; Moore, V. C.; Miller, M. K.; Allen, M. J.; Haroz, E. H.; Kittrell, C.; Hauge, R. H.; Smalley, R. E. *J. Nanosci. Nanotechnol.* **2003**, *3*, 81.
(56) Kumatani, A.; Warburton, P. A. *Appl. Phys. Lett.* **2008**, *92*, 243123.
(57) Krupke, R.; Hennrich, F.; Kappes, M. M.; Lohneysen, H. V. *Nano Lett.* **2004**, *4*, 1395.
(58) Heller, D. A.; Mayrhofer, R. M.; Baik, S.; Grinkova, Y. V.; Usrey, M. L.; Strano, M. S. *J. Am. Chem. Soc.* **2004**, *126*, 14567.
(59) Fagan, J. A.; Simpson, J. R.; Bauer, B. J.; Lacerda, S. H. D.; Becker, M. L.; Chun, J.; Migler, K. B.; Walker, A. R. H.; Hobbie, E. K. *J. Am. Chem. Soc.* **2007**, *129*, 10607.
(60) Park, J.; Butler, J. E. *J. Fluid Mech.* **2009**, *630*, 267.
(61) Al Kahwaji, A.; Kellay, H. *Phys. Rev. Lett.* **2000**, *84*, 3073.
(62) Hoffmann, H.; Hofmann, S.; Rauscher, A.; Kalus, J. Shear-induced transitions in micellar solutions. In *Trends in Colloid and Interface Science*; Springer-Verlag: New York, 1991; Vol. V, pp 24.
(63) Berret, J. F.; Gamez-Corrales, R.; Serero, Y.; Molino, F.; Lindner, P. *Europhys. Lett.* **2001**, *54*, 605.

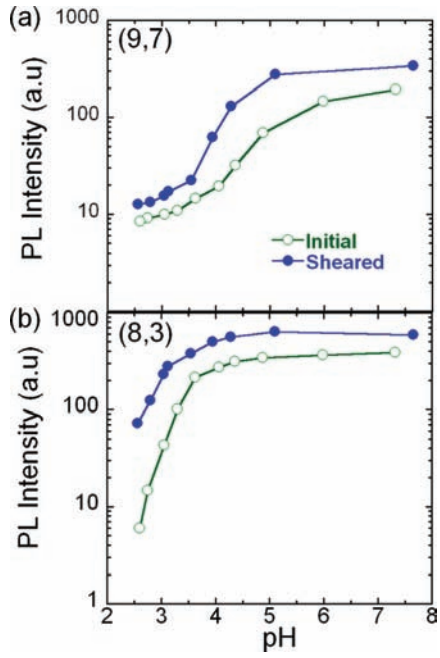

Figure 3. pH-dependent PL intensity of the (a) (9,7) and (b) (8,3) SWNT species in an initial SDS-SWNT suspension and after shearing ($\gamma = 0.4 \times 10^4$ s^{-1}).

high PL intensity as the pH of the aqueous phase is altered. Figure 3 shows that PL intensity from the (9,7) and (8,3) SWNT types in the initial SDS-SWNT suspension decrease by at least an order of magnitude at acidic pH values, similar to previous observations (data for the (9,5) and (6,5) SWNT types are available in Supporting Information).[14,23,24] However, the PL intensity of sheared aqueous SWNT suspensions are less sensitive to the quenching effects of the acid medium. All SWNT (*n*,*m*) types show improved PL intensity at all pH values. The effect is even more dramatic for the smaller diameter nanotubes (e.g., (6,5) and (8,3) SWNTs) at the lowest pH values. At these highly acidic conditions, the intensity from the sheared SWNT suspension remains close to an order of magnitude higher than the initial suspension.

The resistance to quenching suggests that shearing provides a better protective layer around the nanotube. A similar phenomenon was exploited by McDonald et al.[64] to selectively quench the emission of SWNT species based on differences in surfactant adsorption. Better protection of the SWNT from protons also explains the intensity increases to the RBMs of the (9,7) and (10,5) nanotubes in the Raman spectra seen in Figure 2b. These phonon modes are broadened and less intense at high proton concentrations.[24] As the surfactant reorganizes around the nanotube after shearing, the SWNT minimizes its interactions with protons resulting in more intense RBM peaks.

The results shown in Figures 1−3 confirm our previous observation that SDS is capable of suspending large diameter SWNTs; however, SDS is often assembled in a structure that fails to protect the nanotube from extrinsic quenching.[14] Through all-atom (MD) simulations, Tummala and Striolo found that SDS molecules do not spread evenly on the SWNT surface and, at high surface density, prefer to maximize interactions among themselves.[35] Hence, parts of the nanotube sidewall remain exposed to water. Further, there are several reports that suggest

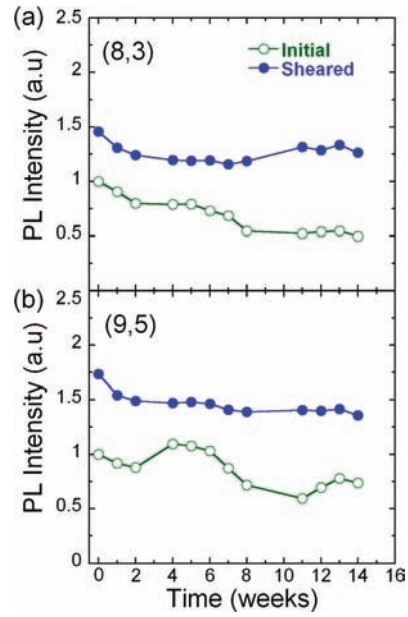

Figure 4. Time-dependent PL intensity of (a) (8,3) and (b) (9,5) SWNT species in an initial SDS-SWNT suspension and after shearing ($\gamma = 0.4 \times 10^4$ s^{-1}).

SDS has lower surface coverage or weaker interactions with large diameter SWNTs.[64,65] These differences in interaction strength may help explain the higher sensitivity of as-prepared SDS-coated SWNTs, especially the large diameter SWNTs, to quenching events. After shearing the initial SWNT suspensions by either the microfluidic channel or rheometer, the surfactant shell acquires a different configuration that provides better protection to the extrinsic factors. This process may be facilitated by shear-induced changes to the micellar structure.[61,62]

Improved Dispersion. The formation of a more robust surfactant structure surrounding SWNTs should also provide larger repulsive forces as nanotubes interact with each other in solution.[66] Therefore, the reorganized surfactant structures should improve dispersion stability. The PL intensity of the initial and sheared ($\gamma = 0.4 \times 10^4$ s^{-1}) SDS-SWNT suspensions were recorded over the course of 14 weeks to measure the dispersion stability, as shown in Figure 4 (data for (6,5) and (9,7) SWNT types are available in Supporting Information). Interestingly, the enhanced PL emission intensity persists for several months. The PL intensity of all SWNT (*n*,*m*) types from the sheared suspension is always higher than that of the initial suspension. Typically, the intensity of the sheared suspension decays slower than the initial suspension. For example, the (8,3) SWNTs in the initial suspension decrease in intensity by 50% (Figure 4a). However, these same SWNT types only decrease by 15% in the sheared suspensions. On the other hand, the behavior of the large diameter nanotubes in the initial and sheared suspensions was different. The intensity from the largest nanotubes (e.g., (9,5) SWNTs) in the initial suspension stayed approximately constant for the first 2 weeks, and then the intensity increased until reaching a plateau (Figure 4b); this observation is attributed to energy transfer from the smaller nanotubes (large band gaps).[20,65] After the sixth week, the

(64) McDonald, T. J.; Blackburn, J. L.; Metzger, W. K.; Rumbles, G.; Heben, M. J. *J. Phys. Chem. C* **2007**, *111*, 17894.
(65) McDonald, T. J.; Engtrakul, C.; Jones, M.; Rumbles, G.; Heben, M. J. *J. Phys. Chem. B* **2006**, *110*, 25339.
(66) Shvartzman-Cohen, R.; Nativ-Roth, E.; Baskaran, E.; Levi-Kalisman, Y.; Szleifer, I.; Yerushalmi-Rozen, R. *J. Am. Chem. Soc.* **2004**, *126*, 14850.

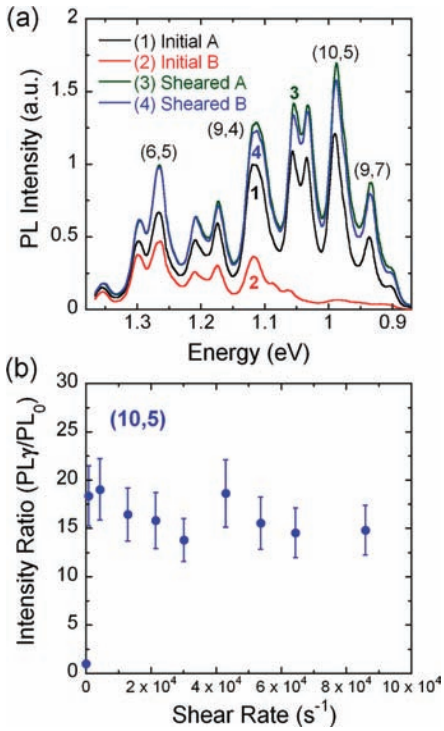

Figure 5. (a) PL emission spectra (ex = 784 nm) from initial and sheared SWNT suspensions. Notice that the initial PL intensity from the larger diameter SWNT species (lower energy) in suspension B are almost entirely absent from the spectra. However, the PL emission intensity of A and B is nearly identical after shearing each suspension. (b) Intensity ratio (PL_γ/PL_0) of the (10,5) species in suspension B as a function of shear rate.

intensity started decreasing again until another period of slow increases is observed after the eleventh week. In sharp contrast, the intensity from the large diameter SWNTs in the sheared suspension stabilized after approximately 2 weeks. The relatively constant intensity from the large diameter SWNTs is attributed to the better surface coverage of the nanotubes with SDS. The results show that shear induces long-term changes to the SWNT PL and aging dynamics of the suspension.

Discrepancies among Suspensions. Although the same dispersion procedure is always used to prepare the suspensions, occasionally SDS-SWNT suspensions show large variations in the initial PL intensity. For example, suspensions A and B (curves 1 and 2) in Figure 5a show a large deviation in the initial intensity of the suspension. The most significant differences are observed for the large diameter nanotubes (lowest emission energy). In suspension B, the large diameter SWNTs are completely absent from the spectra, and the small diameter SWNTs show significant decreases in intensity when compared to suspension A. The first impression from the PL spectra is that suspension B is a "poor" suspension that was unable to adequately disperse the nanotubes. As discussed in Supporting Information, this suspension was bath-sonicated again in an attempt to disperse SWNTs better. This showed marginal improvements to the PL, but the largest diameter SWNTs remained absent from the spectra. Indeed, researchers have often concluded that the largest diameter nanotubes do not suspend well in SDS suspensions.[16] It could also be argued that SWNTs in sample B have a higher defect density causing SWNTs to be optically inactive[67] or that larger SWNTs are in an oxidized nonfluorescing state.[26] However, after both suspensions were sheared at identical shear rates ($\gamma = 0.4\times 10^4$ s^{-1}), the PL emission for both the poor and "good" suspensions increase to the same intensity for all the SWNT species. The most fascinating increases are seen for the peaks corresponding to the (10,5) and (9,7) species in suspension B, which were absent from the initial SWNT suspension spectra. These species show a 20× increase in intensity after the suspension was sheared, as shown in Figure 5b. The similarity in the final PL emission (Figure 5a) and absorbance (Figure S3, Supporting Information) spectra for both suspensions is also significant. Again, these results suggest SDS is capable of suspending large diameter SWNTs; however, extrinsic factors often quench their PL. The effects of extrinsic factors can be minimized by reorganizing the surfactant structure around the nanotube either by shearing the suspension, as shown in Figure 1, or by mixing with organic solvents.[14]

Table 1. Quantum Yields (%) for Selected (*n*,*m*) Species in Sheared Suspensions with PL Intensities That Were Initially Good and Initially Poor[a]

(*n*,*m*)	initially good QY	initially poor QY
(8,3)	0.71	0.88
(9,5)	0.71	0.93
(10,5)	0.88	1.05
(9,7)	0.58	0.66

[a] See suspensions described in Figure 5. More details of quantum yield calculations are given in Supporting Information.

The PL emission intensity increases observed in Figures 1 and 5 occur without significant changes to the absorbance. Therefore, the ensemble QYs of SWNT species has increased considerably after shearing. Table 1 shows QYs calculated for various SWNT (*n*,*m*) types in sheared suspensions by comparison to the dye IR 26 (see Supporting Information). For suspensions that are initially bright, the QYs for the selected species are approximately 0.4%, which are similar to the ensemble values reported by Jones et al.[33] Although Blackburn et al. did not report QYs for SDS-suspended SWNTs, they did comment that QYs were 5 times lower than in sodium cholate suspensions (~1%).[29] As shown in Tables 1 and S2 (Supporting Information), shearing initially good suspensions results in significant increases to the average QY. Although all SWNT species showed improved QYs, shearing had a more significant effect on the larger diameter SWNTs. For example, the (8,3) species initially had a QY of 0.54% that increased to 0.71% after shearing. On the other hand, the (9,7) SWNTs initially had a QY of 0.13% and showed a 4-fold increase to 0.58%. The results are even more impressive for the large diameter SWNTs in initially poor suspensions. The average QY of (10,5) species increases from 0.02% to 1.05% in these SWNT suspensions. Hence, sheared suspensions of SDS-SWNTs show QYs that are comparable to ensemble measurements performed on separated SWNTs[18,68] or SWNTs suspended in other surfactants.[29] An interesting feature of the average QYs calculated in Table 1 is that the initially poor suspensions consistently yielded better final values for the QY than the good suspensions. These results highlight the importance in understanding the surfactant structure surrounding SWNTs since the

(67) Carlson, L. J.; Maccagnano, S. E.; Zheng, M.; Silcox, J.; Krauss, T. D. *Nano Lett.* **2007**, *7*, 3698.
(68) Nish, A.; Hwang, J. Y.; Doig, J.; Nicholas, R. J. *Nat. Nanotechnol.* **2007**, *2*, 640.

PL spectra of as-prepared SWNT suspensions could provide misleading information.[16,26,37]

Shearing Effects on Other SWNT−Surfactant Systems. Preliminary experiments were performed with other surfactants, such as SDBS, SC, and cetyl trimethylammonium bromide (CTAB). Enhancements (∼10%) are observed with SDBS−SWNT suspensions, whereas SC and CTAB suspensions have slight decreases in PL intensity, especially at small shear rates (not shown). However, additional experiments are needed to better understand the behavior of these SWNT−surfactant systems and why SDS systems show such a large increase in PL intensity.

Conclusions

The high-shear forces that SWNTs experience when flowing through microchannels can induce significant increases to the PL of SDS-suspended SWNTs. These PL increases are most significant for the large diameter SWNTs, resulting in PL intensities that can be as much as 2−20 times higher than the initial suspension. The QYs of the sheared suspensions are near 1%, making them comparable to the QYs obtained with sodium cholate. The persistence of the PL and the increased stability of the suspensions suggest that alignment of SWNTs is not responsible. In addition, Raman and absorbance spectroscopy and dielectrophoresis experiments show that disaggregation of bundled nanotubes cannot explain these increases. Therefore, these PL intensity increases are attributed to surfactant reorganization around SWNTs. The ability to alter the surfactant structure demonstrates potential opportunities to further improve PL by tailoring the surfactant structure around SWNTs.

Acknowledgment. The authors acknowledge the Donors of the American Chemical Society Petroleum Research Fund for partial support of this research. C.A.S.-B. thanks SEAGAP at the University of Florida for their support. We gratefully thank Prof. Yiider Tseng for access to the ultracentrifuge, the Richard Smalley Institute at Rice University for supplying SWNTs, and the staff members of UF Nanofabrication Facility (Bill Lewis and Al Ogden) for valuable assistance during the microfabrication of devices.

Supporting Information Available: Flow parameters for the microfluidic channel (flow rates, shear rates and Reynolds numbers), pH-dependent PL, time-dependent PL, calculation of quantum yields, and spectra for SDS-SWNT suspension at different sonication times. This material is available free of charge via the Internet at http://pubs.acs.org.

JA903705K